v1: 27 August 2024

Research Article

Modified Free Energy Generation using Permanent Neodymium Magnet based on Bedini with Maxwell and Lorenz Gauge Conditions

Peer-approved: 27 August 2024

Qeios, Vol. 6 (2024)
ISSN: 2632-3834

Sahar Rahim[1], **Haseeb Ahmed**[1], **Sohail Ahmad**[2]

1. Department of Electrical & Computer Engineering, COMSATS University Islamabad, Islamabad, Pakistan; 2. Independent researcher

An efficient, reliable, and real-time electricity generator is proposed by keeping in view the constraints related to electricity generation cost, resource reservoirs, greenhouse gas emissions, energy storage, and power demand for a pre-defined residential area. Paramount importance is given to the rotor's design, coupled with movable neodymium magnets to increase the harvester's lifespan and the system's net revenue. For the amplification of the stator output, a cost-effective approach is adopted that is based on the parallel winding of the bifilar coil. Furthermore, the coefficient of performance factor for the Bedini's smart school girl circuit-based electricity harvester is modified by aiding the concepts of radiant energy incorporated with the electromagnetic phenomenon. Moreover, the mathematical model is formulated by the Maxwell equations using the Lorenz gauge condition to capture free vacuum energy from the environment. For the investigation, analysis, and corroboration of the proposed design, results are reported after performing extensive numerical computations, and a comprehensive comparison between the original and modified design is stated in detail.

Correspondence: papers@team.qeios.com — Qeios will forward to the authors

I. Introduction

Fossil fuel depletion, global warming, and economic growth are the prominent reasons that drive traditional electric power systems towards the smart power grid with the optimal integration of renewable energy resources and information communication technology (ICT). Over time, the demand for electricity is expected to be amplified at a rate three times that of today. To boost the economy of any country, it is very challenging to cope with such a high demand for electrical energy by just relying on the power grid's old infrastructure [1]. Up till now, non-renewable resources (coal, natural gas, and petrol) are vastly utilized in many countries due to their ease of availability and low purchasing price for the generation of electrical energy, which leads to the diminishing of such resources and also expands the carbon footprint problems. With the advancement in technology, there is a need to save electrical energy and find new methods to consume it in a more efficient manner. Many researchers and scientists have conducted a lot of research and made inventions that have highly influenced electricity tariff rates and the reliability factor, which are affected by high energy losses during the power transmission system. For the sake of a decentralized generation (DG) system, the optimal integration of renewable energy resources (RES) such as photovoltaic (PV) panels, wind turbines, and biogas plants emerges as a global trend to deal with the issues of greenhouse gas (GHG) emissions aimed at preserving non-renewable energy resources [1]. However, due to their volatile and intermittent nature, high integration of the traditional power grid with RES needs a lot of flexibility in the present power network and requires great efforts to achieve maximum efficiency of the grid. For the implementation of the decentralized power system, a Microgrid (MG) is one of the originating ideas; a small electrical network that comprises local power generation sectors with a battery energy storage system (BESS) and flexible consumption schemes, works in plug-and-play mode with the smart grid (SG), and provides resilience, security, and mitigation of grid disturbances in case of a fault [2]. Although it is a great, environmentally friendly, and reliable backup for the electrical power system, synchronization with the main power grid is a difficult task that requires large space and maintenance for storage purposes.

With the evolution in the power generation sector, a lot of research and innovations have been done up till now. Many engineers have toiled on energy harvesters for small-scaled electricity production to fulfill their needs without utilizing conventional resources to minimize energy consumption costs. One of the types of electricity generators produces electrical energy without utilizing any external aid, resulting in zero running cost. Numerous research articles have been published in order to develop a compact and flawless solution to deal with the challenges in the power generation sector. One of the renowned scientists, Nikola Tesla, had first proposed the concept of radiant energy and invented many free energy devices by implementing his unique ideas. By following Tesla's concept, the Bedini generator (another type of electric generator) was invented to generate electrical energy from kinetic energy. In 2001, John Bedini was the first scientist to propose the Bedini simplified schoolgirl (SSG) generator [3][4]. Subsequently, further developments were made by Peter Lindemann and many other researchers [5][6]. Bedini claimed that there is no actual "free" energy; it can be gathered in several ways. The Bedini SSG is a type of electrical generator that consumes the poignant parts of the operational machines to rejuvenate the electrical energy to feed further electric devices or back-up power storage banks. One of the interesting parts of the SSG is the permanent Neodymium (NdFeB) magnets, which are majorly applied in free energy motors owing to the reason that they do not easily lose their magnetic power (the demagnetization power is 1% after one-fourth part of the decay). As compared to other types of magnets, the strength and power of the permanent magnet are high and do not need power for magnetic field generation [7]. Fig. 1 illustrates Tesla's idea, which involves the procedure of atmospheric energy capturing for over-unity machines.

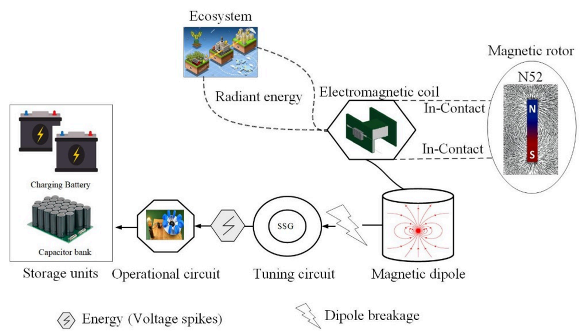

Figure 1. Conceptual diagram for Tesla's idea

It is depicted that electromagnetic coils capture radiant energy from the environment and also play a crucial role when the rotor of the magnetic motor rotates and all its embedded permanent magnets come into contact with these coils at an angle of 90° degrees. As a consequence, the magnetic dipoles are created and stored in each coil fixed on the stator part. According to the SSG tuned model, whenever these dipoles are broken, the energy in the form of high voltage spikes is produced that can be easily stored in energy storage systems through switching circuits and filters to fulfill the electricity demand.

A. Literature review

In the literature, the magnetic motor is one of the hot research domains for generating electricity since the 18th century. Numerous free electrical energy generation techniques have been proposed to achieve a socio-economic and user-friendly source of electrical energy. In this context, some of the most recent, state-of-the-art, and related research is highlighted and summarized here. In [8], J. Jines' permanent magnet motor was invented based on selective and adjustable shielding of the drive magnets arranged in two staggered annuli to produce a continuous force in one direction for the proper mechanical arrangement, causing the rotor's rotation and driving a power shaft coupled with a speed regulator of the motor and power shaft. Another permanent magnet motor is designed in which pairs of permanent magnets are normally placed in a repulsive state (utilized as the power source) while the magnetic shield mechanism between the magnet pairs is adjusted for the power outage maximization [9]. H. Johnson invented a permanent magnetic motor in [10] using the natural and instinctive behavior of the permanent magnetic phenomena (attraction and repulsion) to create a rotational motion for a motor's long period. Accordingly, it runs due to the utilization of unpaired electron spin in a permanent ferromagnetic without any electricity input. Patent [8] presents the permanent magnet motor established on the permanent magnet's position while the interaction is controlled by implanting a coil in the vacuum between magnets, which in return is capable of a large amount of output (energy and torque) generation. [4] proposed a back electromagnetic force (EMF) monopole motor comprised of a rotor mounted with magnets in a monopole condition. When momentarily in apposition with a stator's magnetized coil's piece with three winding coils (power, trigger, and recovery), the back EMF energy is rectified by a high voltage bridge to transfer energy to a high voltage capacitor for storage in a recovery battery. A magnetic motor is fabricated by applying the magnetic coupling shaft phenomena in a master and slave assembly for the implementation of Victor Diduck's permanent magnet motor [11]; slave wheels and magnets at a specified angle to generate power, whereas both drive and slave magnets are magnetically coupled with a like-faces-like orientation poles arrangement.

A Chinese author in [7] constructed an electric generator (with 5 kW), powered by permanent magnets without running fuel. Its motor consists of a four-armed rotor placed in a shallow bowl of liquid with colloidal suspended magnet particles and has two cylinders (inner rotating and outer fixed). By adjusting the north pole's magnetic alignment, the inner cylinder will face magnetic repulsion that keeps the rotor's acceleration to store energy. Martin et al. claimed that a free energy generator based on Tesla's concept would work with more than 100% efficiency. Using the relationship between speed and torque, they determined the efficiency of Adam's electric motor-generator set, a motor that is built and demonstrated to run without any input and utilizes the energy stored in the atoms of permanent magnets [12]. A bearing-less motor is developed in [13] that can realize magnetic levitation rotations without any mechanical contacts by adopting a distributed winding to suppress the iron losses, while the neodymium sintered permanent magnets are attached to achieve a maximum power density. Ali and Ismail projected a self-rotated magnetic motor in which the rotor is naturally in the state of the magnetic field's repulsion and attraction by arranging all the magnets into a Halbach array for free electric energy production [14]. Also, it is known as a machine that generates free electric energy with the self-rotating rotor and rotates at a constant speed to produce a torque that leads to mechanical power development.

During the 21st century, the escalating concerns over electrical energy security owing to the depletion of fossil fuels, the progress in free energy sources has gained more interest in all accessible alternative energy forms. In 2006, an Irish company, "Steorn Ltd," announced the development of free, clean, and constant electricity through magnetic interaction via an over-unity device with eight ferrite rings mounted on the stator and eight pairs of permanent magnets embedded on the rotor; however, the feasibility of the motor is not known yet. M. Yildiz invented a permanent magnet motor with an over-unity characteristic in which alternating magnetic field generation interacts with a stationary magnetic field with an estimated output of 250W [15]. In [16][17], the authors presented a comparative analysis of two types of Bedini SSG generators: the original Bedini monopole SSG energizer and the 4-pole Neodymium magnet Bedini SSG. They studied the assembly and performance of the original Bedini and its replica design to evaluate the battery's coefficient of performance (CoP). The results show that the replica design charges faster with less power consumption and improves the CoP to about 8% as compared to the original one.

Photong et al. worked on the effects of stationary coil size on the power generation capability and discussed the effects of four diverse coil sizes (20, 21, 22, and 23 AWG) on the power generation through the Bedini generator in [18]. The operation of the battery running and charging in the original design is compared with the performance of the DC-DC boost converter, which offers capabilities of greater voltage boost to enhance the step-up power conversions in the six-pole and eight-Neodymium magnet generator prototype that potentially provides free energy to calculate the CoP for the battery performance of both designs [19]. [20] analyzed a radiant charger as a free energy device to produce electricity with a prototype using five coils and five neodymium permanent magnets.

B. Contribution

In this paper, the original model of the Bedini generator is compared with the proposed modified free energy generator (MFEG). The MFEG's performance is evaluated, and several tests are performed to calculate the coefficient of performance (CoP) that provides a radiant energy transfer measurement and is defined by the output in proportion to the input operators. In the proposed prototype, a concise and automatic model for the free power generator is presented to overcome the crisis of electrical energy deficiency, uncertain distribution system, load shedding, and carbon footprints. MFEG is also based on the concept of the Bedini SSG generator. Moreover, its functionality is totally different from conventional generators that consume a large amount of input fuel, have a limited lifespan, and cause environmental pollution. Our contributions are enlisted as,

- Rotor designing using the best quality neodymium magnets; runs in an autonomous mode without any fuel consumption.
- Construction of the stator using bifilar coils (BC) as the interaction of permanent magnets and BC to capture radiant energy is one of the key fragments in MFEG.
- Assembly of modified tuned SSG circuits by adjusting the gaps between magnets and coils.
- Calculating regarding CoP of the selected batteries for the sake of performance comparison between the Bedini generator and MFEG.

Our article is further organized as follows: the mathematical model is proposed in section II, detailed design and operation are explained in section III, whereas the working principle and flowchart are presented in section IV. Section V discusses the analysis and comparison of performance to express the validation of our scheme. In the end, the conclusion is stated to summarize our work in section VI.

II. Mathematical Model

In our proposed work, the design and construction of the rotor, stator, and Bedini SSG are crucial parts. All of these parts must be built and assembled with accurate materials, chosen based on quality and cost. The state-of-the-art methodology, implementation, and selected materials will yield positive results; highly beneficial for the evolution of free energy generation. NdFeB magnets are mounted on the rotor's circumference, embedded at equal distances from each other with opposite polarities. BCs are wound spools and fixed on the stator to be precisely aligned with each magnet at an angle of 45°, comprised of two counter and highly conductive coils [18]. Each turn of the coil produces a maximum potential difference between adjacent turns to get high energy (relates directly to the square of the potential difference of adjacent turns). Energy storage systems such as batteries must be examined while fabricating SSG circuits. To enhance the efficiency of the Bedini SSG circuits, improvement in CoP is one of the key factors. It is applied to any machine that utilizes energy from its surroundings having a value greater than one. The conceptual layout of the intelligent power generator involves two different input energy sources, as shown in Fig. 2.

doi.org/10.32388/OS9V96.2

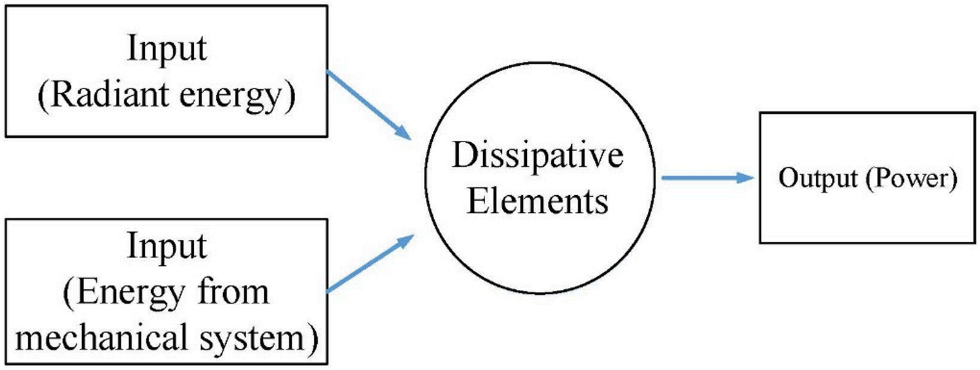

Figure 2. The visionary model for MFEG.

A. Maxwell equation

For the design and construction of the presented motor, Maxwell's equations subjected to Lorenz gauge conditions have been considered to thoroughly understand the phenomenon by which the radiant energy is captured and utilized from the vacuum [21]. In our system model, energy from the vacuum is very critically analyzed, reliant on the self-consistent set of Maxwell equations to achieve the desired objective (CoP>1).

1. Electric Gauss's Law

The first Maxwell's equation is adopted to estimate the quantity of enclosed charges by mapping the electric field exterior to the charge distribution for the assessment of electric field strength.

$$\nabla.\overrightarrow{E}=\frac{\rho_o}{\epsilon_o} \tag{1}$$

Here, $\overrightarrow{E}$, ρ_o, and $\epsilon_o$are the electric field strength, charge density, and free space permittivity, respectively.

2. Ampere's Law

To calculate the magnetic field around BCs, which are current-carrying coils, Ampere's law is employed. Its differential form is stated as follows,

$$\nabla\times\overrightarrow{B}=\mu_o\left(\overrightarrow{J}+\epsilon_o\frac{\partial\overrightarrow{E}}{\partial t}\right)=\sigma\overrightarrow{E} \tag{2}$$

where, $\nabla\times\overrightarrow{B}$ is the driving force, σ is the vacuum's conductance, $\overrightarrow{J}$ is the vacuum's electric charge density, and $\frac{\partial\overrightarrow{E}}{\partial t}$ is the rate of change in electric charges in free space.

3. Faraday's law of Induction

For the predicted amount of electromotive force as a result of interaction between the magnetic field and electric circuit (SSG), the following equation is considered,

$$\nabla\times\overrightarrow{E}=-\left(\frac{\partial\overrightarrow{B}}{\partial t}\right) \tag{3}$$

$\overrightarrow{E}$ is the electric field lines flow only when there is a change in magnetic flux concerning time.

4. Gauss's Law of magnetism

This law has been used as a constraint to check the absence of free magnetic poles such that if there is the existence of magnetic monopoles, then the total flux through a closed surface must be equal to zero.

$$\nabla.\overrightarrow{B}=0 \tag{4}$$

B. Lorenz gauge transformation

By introducing the potential vector $\overrightarrow{A}$, all the above-mentioned equations are transformed into two simplified potential equations by following the Lorenz gauge concept [22]. The set of two equations is given as,

$$\nabla^2V+\frac{\partial}{\partial t}\left(\nabla.\overrightarrow{A}\right)=-\frac{\rho_o}{\epsilon_o} \tag{5}$$

 doi.org/10.32388/OS9V96.2

$$(\nabla^2 \overrightarrow{A} - \mu_o \epsilon_o \frac{\partial^2 \overrightarrow{A}}{\partial t^2}) - \nabla(\nabla.\overrightarrow{A} + \mu_o \epsilon_o \frac{\partial V}{\partial t}) = -\mu_o \overrightarrow{J} \tag{6}$$

Here, V is the electric potential variable. According to Lorenz gauge transformation conditions [23], the parameter $\overrightarrow{A}$ is $\nabla.\overrightarrow{A} = -\mu_o \epsilon_o \frac{\partial V}{\partial t}$ and the d'Alembertian operator is $\boxdot^2 \equiv -\mu_o \epsilon_o \frac{\partial^2}{\partial t^2}$. Then the equation (5) and equation (6) reduce to,

$$\boxdot^2 = -\frac{\rho_o}{\epsilon_o} \tag{7}$$

$$\boxdot^2 \overrightarrow{A} = -\mu_o \overrightarrow{J} \tag{8}$$

$\overrightarrow{J} = \sigma \overrightarrow{E}$ is the conductance at the vacuum (analogous to Maxwell displacement current). According to T.D Lee [24], vacuum is a stage of minimal energy from the environment, also called zero-point as an energy state. Thus, by considering $\rho_o = 0$ and $\overrightarrow{J}$ =0, the Maxwell's equations are,

$$\nabla.\overrightarrow{E} = 0 \tag{9}$$

$$\nabla \times \overrightarrow{B} = \mu_o \epsilon_o \frac{\partial \overrightarrow{E}}{\partial t} \tag{10}$$

$$\overrightarrow{H} = \frac{1}{\mu_o} \overrightarrow{B} + \overrightarrow{M} \tag{11}$$

$$\nabla.\overrightarrow{B} = 0 \tag{12}$$

Here; $\overrightarrow{H}$ and $\overrightarrow{M}$ denote magnetic field strength and magnetization, respectively. All of the above Maxwell equations include the vacuum's effect used for the design and operational principles of our schematics of the energy harvester.

III. Design and Operation

Based on the concept of Nikola Tesla, MFEG is implemented by following the resonant inductive coupling principle [25]. In our paper, a cost-effective and novel approach is adopted that can efficiently transfer vacuum energy into mechanical energy. Afterward, it is converted into electric power that could be supplied to the MGs or could be stored in BESS to ensure the reliability and security of the power grid. In the following parts, the details of the selected components are enlisted below;

A. Rotor

It is noteworthy that a non-magnetic and round-structured rotor is employed, and the acrylic glass frame holder, which remains unaffected by the magnetic field, is used. In our case, eight magnets are mounted at a suitable distance on the mechanical part to design eight monopole rotors by keeping in view the principle of Lorentz force. For precautionary measures, heavy-duty strapping tape is wrapped around the rotor's perimeter to avoid the gluing of the magnets. Additionally, a ball bearing is deployed for the rotation of the rotor around its axis, causing smooth, balanced, and low friction in the rotor. A simplified rotor design is given in Fig. 3.

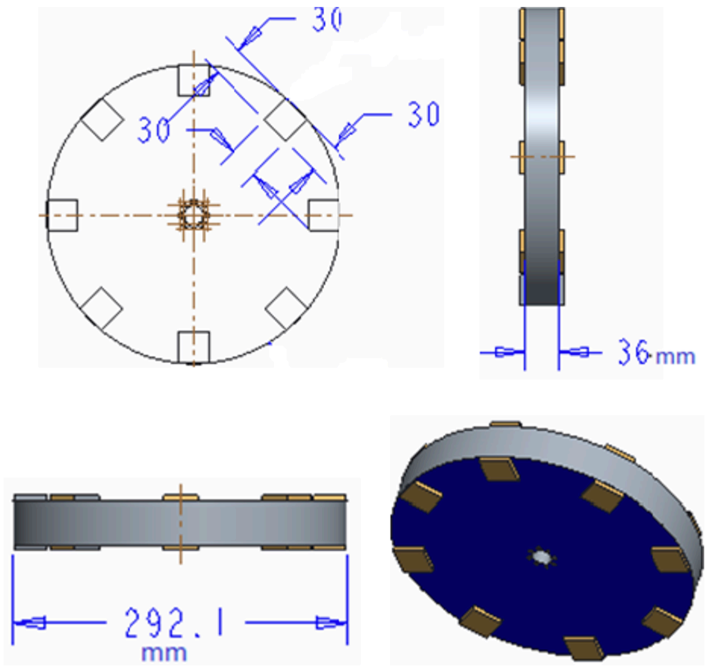

Figure 3. Rotor design

Nickel-coated rectangular-shaped Neodymium magnets of N52 grade (one of the strongest and rare magnets globally used in electric motors due to their higher remanence and coercivity [7]) are employed on the rotor. To avoid the intersection of the scalar south pole, each magnet is placed at 45°, and the distance must not be less than 1.5 to 2 magnet width sizes. The pictorial design can be visualized in Fig. 4.

doi.org/10.32388/OS9V96.2

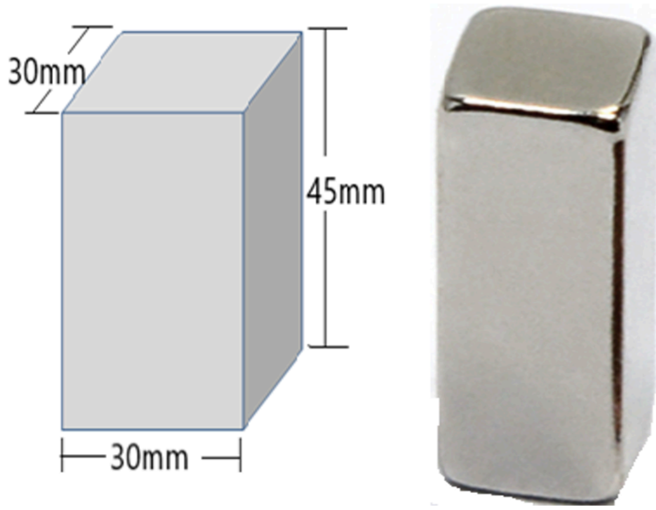

Figure 4. Neodymium magnet's dimensions

B. Stator

An acrylic plastic sheet is used for the stator's structure. BC is wound on the plastic frame called a bobbin or spool, fixed on the stationary part at a specified distance from each other as shown in Fig. 5. Coil selection is important for an efficient system; the larger the diameter, the lower the resistance R and the higher the power transfer absorbance such as absorbance as $P = \frac{V^2}{R}$. The MFEG's spool is comprised of two copper windings in the parallel configuration: slave coil or trigger coil (TC) and power coil or master coil (MC) with different standard wire gauges (SWG). BC is considered the main part when connected to the SSG to produce electromagnetism [4].

doi.org/10.32388/OS9V96.2

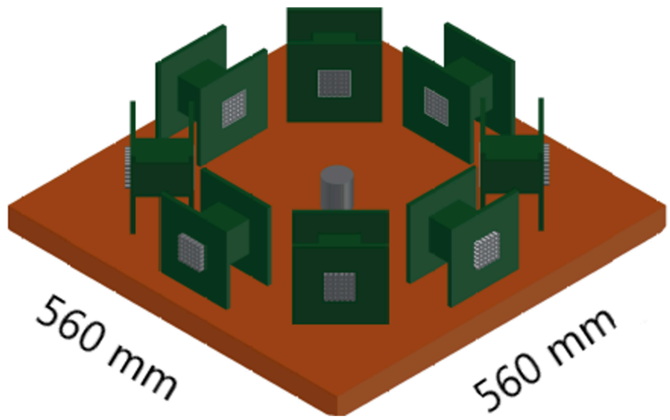

Figure 5. Stator design

Moreover, the spool's core window is laminated with welding electrodes to avoid eddy current losses; its filling factor is normally less than 1. In our model, the core with filling factor Kw < 50% is used. Furthermore, the induced voltage per turn for each spool can be adjusted according to the desired power rating by using the following equation [26],

$$\frac{Volts}{turn} = 4.44 \times f_c \times \xi_c \times A_c \tag{13}$$

Here, f_c is the frequency that depends on the protocol of a particular country (either 50 Hz or 60 Hz), $\xi_c$is the electromagnetic flux density, and its standard value is based on the material type, and Ac is the cross-sectional area for each coil. Furthermore, the coil's size is formulated in accordance with the stator winding's power by the following formula.

$$Size = \frac{\sqrt{V_d \times I_d}}{5.58} \tag{14}$$

V_d, I_d, and 5.58 are the desired voltage, current, and constant values used in our model for the coil core. The design of the BCs wound on the former is shown in Fig. 6.

doi.org/10.32388/OS9V96.2

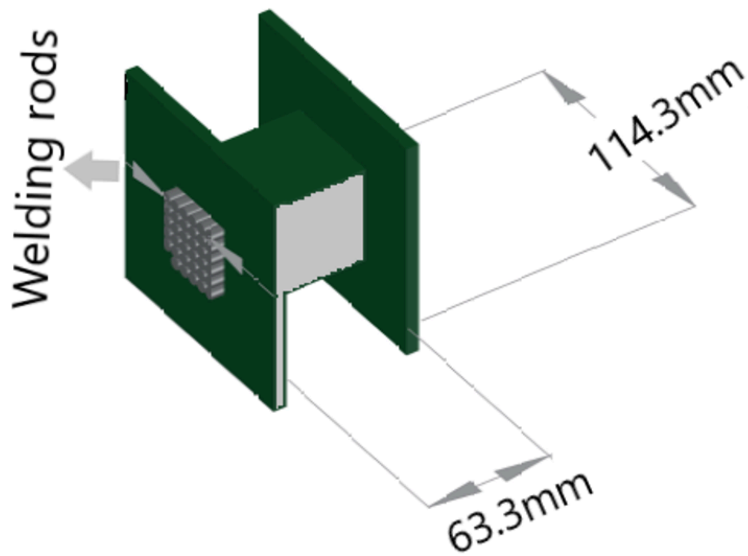

Figure 6. MFEG's Spool

Details and specifications of the components in the Rotor and Stator are given in Table 1.

doi.org/10.32388/OS9V96.2

Items	Material	Dimension
Rotor Disk	Acrylic Plastic	(292.1×292.1) mm
Bifilar Coil	8(Plastic Material)	(1.5×1.5) mm
Magnet	N52	$(30 \times 45 \times 30)$ mm
MC	Copper #20 AWG	2kg (20 AWG)
TC	Copper #22 AWG	2.5kg (22 AWG)
Battery	Lead Acid	12V, 12A (AH)
Bearing	Ball bearing	JWB-3085

Table 1. Rotor and Stator components

C. SSG circuit

Fig. 7 illustrates the basic working principle of the Bedini SSG circuit. In the SSG circuit design, transistors are used for switching purposes, playing a vital role in the created dipole breakage and producing high voltage spikes.

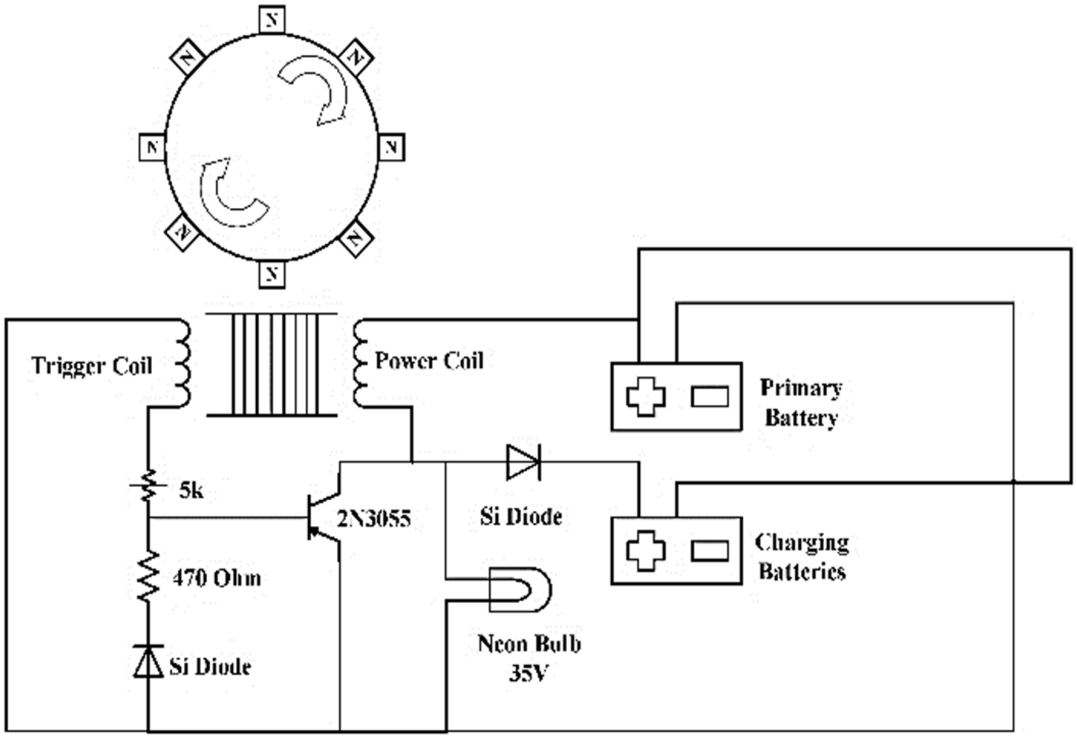

Figure 7. Operational circuit for Bedini SSG

Whereas the resistor is placed before the base of the transistor to provide circuit protection in case of overcurrent conditions, and silicon diodes with a voltage drop of 0.7V are applied to avoid the current's backflow. All of the eight SSG circuits are attached against each bobbin at the stator for dipole formation, while voltage filtration is done by using capacitors. A neon bulb is employed as a circuit breaker; whenever any undesirable situation occurs, it burns out to cut off the current passage. With the help of a variable resistor, the speed of the MFEG's rotor can be adjusted. Furthermore, the specifications and values of the SSG's components are enlisted in Table 2.

- **Battery:** One of the most important components of our project is the electrical energy storage system. For the sake of experimentation and analysis, lead-acid batteries are used in our design. Following the capability of discharging and recharging, batteries are categorized into two groups; named primary and secondary batteries. In the charging battery, the phenomenon of charging will be performed, while discharging will be done at the primary battery. Charging and discharging both functions are performed simultaneously for each Bedini's SSG circuit. It is vital to determine the CoP of the lead-acid battery; the charging battery is discharged with a load and again charged with the support of charging the battery.
- **Tuning tests:** Two tests are performed for the tuning of each SSG circuit, briefly discussed here,
  - **1Ω resistance test:** Performed by first disconnecting the primary battery and measuring the base resistance *($R<1$),* afterward, checking the voltage across the neon bulb *($V\leq 1V$),* as per our model's specification. If the voltage is greater than 1V, the neon bulb will be destroyed.
  - **Sweetspot test:** It is defined as a point where the highest revolution per minute (RPM) of the rotor is achieved with a lower current drawn from the primary battery. For tuning the base resistance and to find the sweetspot point, it is advisable to use a potentiometer. In our case, the sweetspot point is attained using a 427 Ω resistance.

doi.org/10.32388/OS9V96.2

Components	Specification	Value
Transistor	Type	NPN
	Model	2N3055
	Vmax B to E	7V DC
	Vmax C to B	100V DC
	Temperature	$(-65 \sim 200)$℃
Diode	Type	Silicon
	Model	1N4001, 1N4007
	Power Dissipation	0W, 3W
Capacitor	Voltage	50V
	Capacitance	100 μF
	Tolerance	20%
Resistor	Resistance	$1\Omega,\ 470\Omega$
	Power Rating	1 W
Neon Bulb	On-state Color	Red
	Current	(0-30) mA
	Life	30000 h
Welding electrodes	Company	Spark
	Model	AWS-E6013
	Current	$(60 \sim 90)A$
	Voltage	$(50 \sim 80)V$
	Size	6.3 mm

Table 2. Components of SSG circuits

In the following section, a comprehensive discussion about the operation and flowchart for the construction of MFEG is presented.

IV. Working Principle

In our prototype, a permanent magnet generator is designed to run with the minimum initial energy from the primary battery and acquire full RPM within less time. According to equation (9)-equation (12), environmental energy is captured in the rotor-stator and stored in the charging battery. The MFEG's schematic with CoP>1 is displayed in Fig. 8. It is a horizontal system in contrast to the original Bedini design.

M_1, M_2, M_3, M_4, M_5, M_6, M_7, $and\ M_8$ are eight N52s attached at the pre-defined angle on the rotatory part, whereas BCs, further consisting of MC and TC, are properly devoted to the stator and aligned with magnets. Such that the SSG circuit is placed against each BC for the utilization of the radiant energy that is captured by BC. Electric potential is created due to magnetic flow in the MC and TC at the ends of the windings. The voltage value at the spool ends is dependent on the rate of change in flux, therefore proportional to the N-pole rotor's speed. One of the unique features is that a small input energy for the biasing is initially provided, then the MFEG's system works automatically without any external aid and also maintains the rotor's RPM. When the rotor passes through the spool's coil, voltage is generated in the TC winding; it gets the positive signal to switch on the transistor. The triggering signal's intensity is controlled by a neon bulb, while the current is limited by passing it through the potentiometer and connected resistor. The bulb glows (dimly) when the SSG circuit is tuned correctly (useful operation's indication). Thus, the triggering circuit turns on the bases of each transistor. During the conduction state, the back flux is produced, and energy is consumed from the primary battery. This magnetic flux is opposite to the N-pole generated flux to overcome the primary flux generated by the magnet and, as a result, speeds up the rotor.

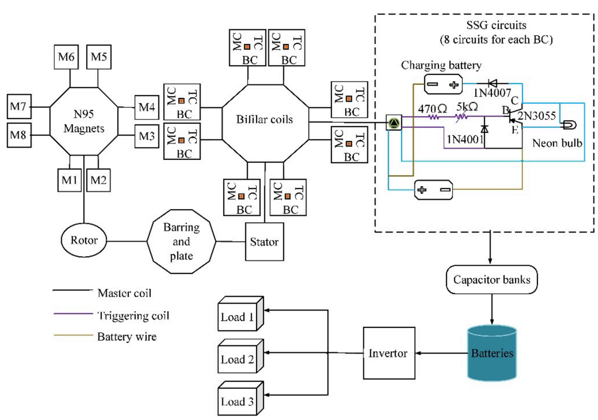

Figure 8. Proposed MFEG's schematic

It will magnetize the electromagnetic core, thus creating an N-pole bobbin on the stator that repels the rotor's N-pole. By controlling the winding, the back flux becomes larger than the winding flux, and the voltage polarity at the TC ends changes and starts decreasing until the transistor is switched off. Because of the commutation, sharp pulsed power, MC's current, and sudden cut-off, the coils can raise the voltage across their ends very rapidly and drag the transistor's collector voltage up to several hundred volts. This effect is due to the energy from the environment (unlike conventional electricity). Moreover, the voltage rise effectively turns on the silicon diodes; it feeds the excessive free energy (high gradient pulses) into the charging battery. Bedini SSG circuits give the possibility to collect the energy of electrons and ions from the vacuum, and pulses are terminated according to the Lenz law. This energy harvester operates by pulling in the environment's power and feeding it to the charging battery. The drawing in of the power can be disrupted if any attempt is made to loop the vacuum's energy back to the system. However, in case of battery failure, MEFG still works either by getting electricity from external sources or the battery is charged through the feedback system using the static relay to the SSG circuits. The capacitor banks are used to improve the power factor and are attached to the BESS through connectors. Afterward, inverters are attached to convert DC into AC following the signals from the control box for the electricity distribution substation among connected loads. The overview of steps involved in the construction of MFEG is displayed in Fig. 9.

doi.org/10.32388/OS9V96.2

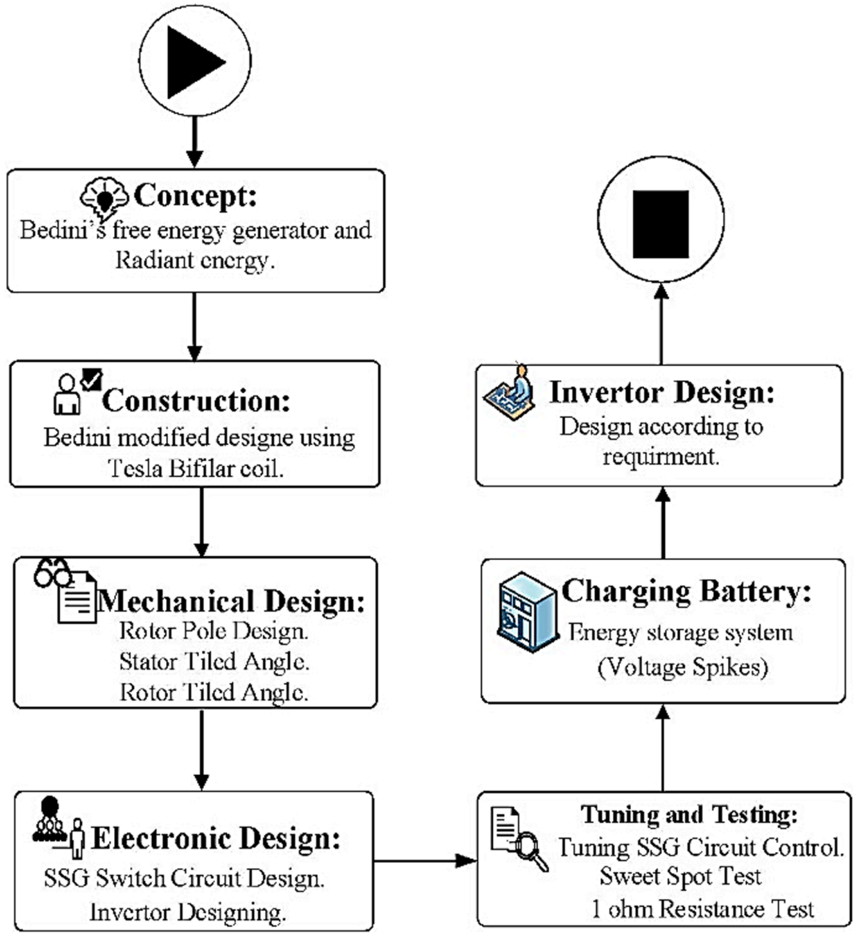

Figure 9. Flowchart of MEFG

V. Performance Comparison

We have done extensive computations and test analyses to verify the performance of MEFG. For the simulations, two professionally developed software programs (Pro-engineer and MATLAB 2017a) are used on a computer with the specifications: Windows 10 (64 bit), Intel (R) Core(TM) m3-7Y30 (7th Generation) i7, CPU@ 1.00 GHz, 1.61 GHz with 8.00 GB installed memory. From the results, it is clear that the RPM of the proposed MEFG energy harvester is much higher than the original Bedini generator. Thus, the time taken for charging the battery in the original design is much greater as compared to the modified one; due to the feedback speed control system of the modified rotor, the charging rate of the battery is increased with the rotor's RPM. After the comparison between the two designs, we extract notable results, presented in a bar chart in Fig. 10. The graph shows how much power is consumed while rotating the rotor and the energy generated by the rotor in both designs. The power consumed by the MFEG is much less than the original design because the torque produced by MFEG is less as compared to the original one. Thus, the battery's power consumption is reduced by low torque, and high RPM transfers high power to charge the batteries in our presented model. We used the CROWN micro "CBT-12-12" lead-acid battery for the reliable storage of generated electrical energy, having silent features of high reliability, a service life of at least five years, standard package size, standard type terminals, and is highly suitable for energy storage banks [30]. To test the efficiency of the system, CoP is used, which is a scientific terminology usually applied to electrical systems in which additional input operating power is taken from the environment. It is mathematically expressed by the following formula [27][28].

doi.org/10.32388/OS9V96.2

$$CoP = \frac{P_{out}}{P_{in}} \tag{15}$$

Here, the output energy can be found out by $P_{out} = V_{avg(out)} \times I_{load} \times t_d$ and input energy is calculated by $P_{in} = V_{avg(in)} \times I_{in} \times t_c$ over the discharging t_d and charging time t_c, respectively.

doi.org/10.32388/OS9V96.2

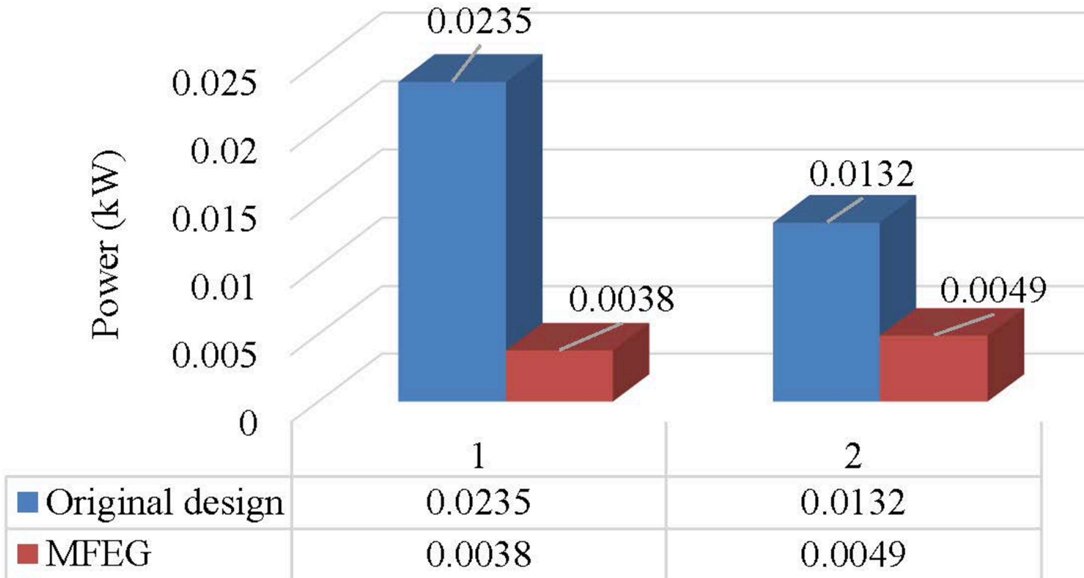

Figure 10. Comparison between original design and MFEG

After extensive experimentation and analysis, results are presented in Table 3. Both energies (input and output) are taken in Joules, and it is noticed that the CoP for both systems (original design and MFEG) is greater than 1. Moreover, the CoP for the proposed model is much greater than that of the original generator; after six cycles, the average CoP of MFEG is 1.836, much larger than 1.470, the average CoP of the original design. Therefore, we can significantly claim that our generator, MFEG, absorbs more power transfer during one time period as compared to the original design due to dual input energies, and also its running cost is approximately equal to zero. A comparative bar chart is shown in Fig. 11 that depicts our outcomes for CoP calculation.

doi.org/10.32388/OS9V96.2

CoP	Input energy (Joule)				Output energy (Joule)			
	I_{in}	$V_{avg(in)}$	t_c	P_{in}	I_{load}	$V_{avg(out)}$	t_d	P_{out}
	A	**V**	**s**	**J**	**A**	**V**	**s**	**J**
Original Design								
1.274	0.392	12.180	8674	41414.533	0.860	12.300	4,988.960	52773.219
1.614	0.396	12.260	28,790	139774.298	0.830	12.370	21,978.100	225651.351
1.437	0.401	12.480	45,982	230115.999	0.840	12.540	31,401.450	330770.313
1.474	0.440	12.340	52,060	282664.976	0.820	12.430	40,878.350	416656.670
1.601	0.467	12.290	64,400	369619.292	0.830	12.530	56,922.400	591987.268
1.420	0.490	12.460	78,800	481105.520	0.850	12.550	64,079.600	683569.133
Average CoP = 1.470								
MFEG								
1.768	0.092	12.950	8674	10334.204	0.280	13.080	4,988.960	18271.567
2.030	0.098	12.990	28,790	36650.246	0.260	13.020	21,978.100	74405.978
1.787	0.112	13.040	45,982	67155.791	0.290	13.180	31,401.450	120022.622
1.596	0.119	13.110	52,060	81218.285	0.240	13.210	40,878.350	129600.721
2.041	0.126	13.200	64,400	107110.080	0.290	13.240	56,922.400	218559.247
1.793	0.162	13.230	78,800	168888.888	0.320	13.310	71,079.600	302742.232
Average CoP = 1.836								

Table 3. Results for the Original and MFEG design

From Fig. 12, it is clearly shown that the primary and charging battery for MFEG allows greater power transfer as compared to the original design, which validates the claim of our model. This is due to the speed of the rotor, the rate of change in magnetic flux, and the SSG circuits being properly tuned to get maximum power from the environment. The proposed prototype for MFEG is not only efficient in terms of output power and CoP but also economical. This is due to the smart power electronic components used in the construction of SSG and control boxes, such as switching circuits, the structure of the rotor/stator, batteries, and spool formation. For the sake of comparison, the data for the Bedini generator is taken from [29] and compared with MFEG in Table 4.

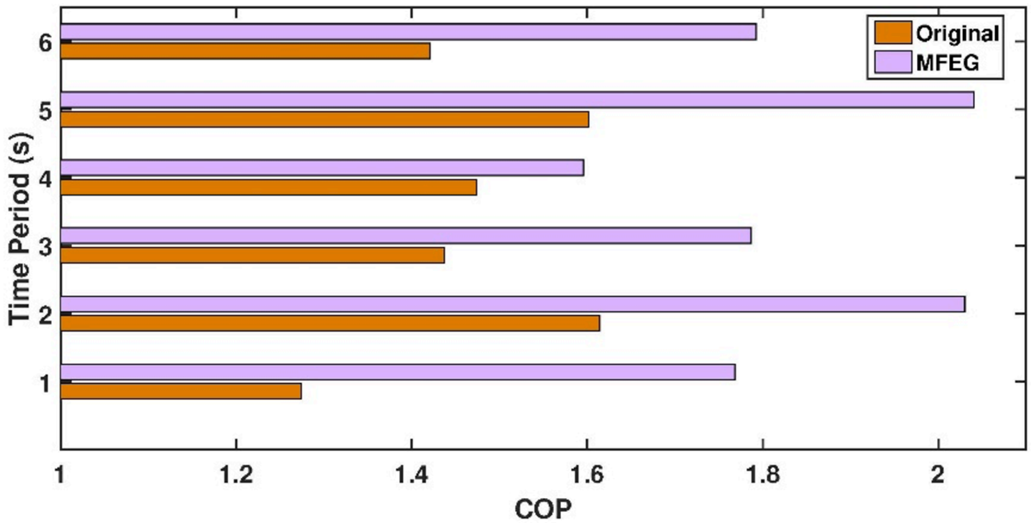

Figure 11. CoP chart

doi.org/10.32388/OS9V96.2

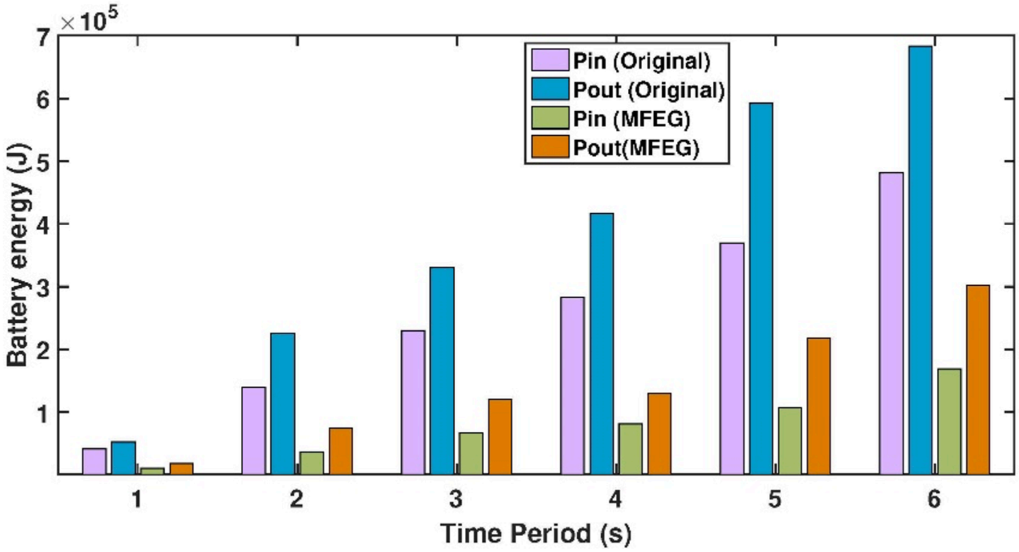

Figure 12. Battery's power

doi.org/10.32388/OS9V96.2

Type	Equipment	Capacity	Cost
Bedini	Multivibrator circuit	Empower home electric utensils	559$
	Amplifiers		
	Motors		
	Battery		
	Electromagnets		
	Miscellaneous		
	Shaft		
	Body parts		
MFEG	Switching circuit	Empower home electric utensils	488.28$
	Batteries		
	N52		
	Miscellaneous		
	Shaft		
	Body parts		

Table 4. Estimated cost

VI. Conclusion

Our MFEG has significantly improved the CoP by about 20% due to its novel combination of the Bedini motor and radiant energy. From the comparison analysis between the two models (original and MFEG), we concluded that our model has minimized its input battery consumption and maximized the output power by adjusting the BC's angle and the number of turns in the bobbin. Besides that, our generator can charge energy storage faster than the original design and also consumes less power. By using advanced electronic devices, the construction cost of MFEG is less than the original design; approximately, we have saved 12.65% in cost while its running cost is near zero. Moreover, due to the N52 magnet, the lifespan of MFEG is much longer than the original design. This new design is small-scaled, user-friendly, economical, and efficient in terms of performance with a reduction in environmental pollution.

In the future, we will focus on the structure of the rotor and control box to generate and manage the bulk of power during electricity generation and distribution with minimum power losses. Also, to enhance the speed of the rotor, we will use artificial intelligence techniques and design a self-healing circuit.

References

1. [a, b] *S. Rahim, N. Javaid, A. Ahmad, S. A. Khan, Z. A. Khan, N. Al- rajeh, and U. Qasim, "Exploiting heuristic algorithms to effi- ciently utilize energy management controllers with renewable energy sources," Energy and Buildings, vol. 129, pp. 452–470, 2016.*
2. [^] *A. Halu, A. Scala, A. Khiyami, and M. C. Gonza´lez, "Data- driven modeling of solar-powered urban microgrids," Science advances, vol. 2, no. 1, pp. e1500700, 2016.*
3. [^] *S. Rahim, N. Javaid, R. D. Khan, N. Nawaz, and M. Iqbal, "A convex optimization based decentralized real-time energy management model with the optimal integ*

ration of microgrid in smart grid," Journal of Cleaner P roduction, vol. 236, p. 117688, 2019.

4. a, b, c J. C. Bedini, "Device and method of a back emf per manent electromagnetic motor generator," US Patent 6,392,370, May 2002.
5. ^ J. C. Bedini, "Device and method for utilizing a mono pole motor to create back emf to charge batteries," US Patent 6,545,444, Apr. 2003.
6. ^ L. G. Sapogin and Y. A. Ryabov, "Low energy nuclear r eactions (lenr) and nuclear transmutations at unitary quantum theory," Int. J. Phys. Astron, vol. 1, no. 1, pp. 14 –29, 2013.
7. a, b, c P. RajaRajeswari, S. Sakthi, K. Bharathi, M. Sasiku mar, and S. Srinivasan, "Zero-point energy conversion for self-sustained generation," J. Eng. Appl. Sci, vol. 10, no. 10, pp. 4326–4333, 2015.
8. a, b C. J. Flynn, "Magnetic motor construction," US Pate nt 5,455,474, Oct. 1995.
9. ^ J. E. Jines and J. W. Jines, "Means for shielding and uns hielding permanent magnets and magnetic motors ut ilizing same," US Patent 3,469,130, Sep. 1969.
10. ^ H. R. Johnson, "Permanent magnet motor," US Patent 4,151,431, Apr. 1979.
11. ^ V. Diduck, "Magnetic motor," US Patent App. 11/781,89 3, Dec. 2007.
12. ^ M. Koutny´, P. Kacˇor, P. Bernat, and T. Pavelek, "FEM electromagnetic simulation and operational testing of the adams electric DC motor-generator," Conf. in ELEK TRO, pp. 325–330, May 2016.
13. ^ Y. Fu, M. Takemoto, S. Ogasawara, and K. Orikawa, "I nvestigation of a high speed and high power density b earingless motor with neodymium bonded magnet," i n IEEE Int. Elec. Mach. and Drives Conf. (IEMDC), pp. 1 –8, May 2017.
14. ^ A. H. Ali and A. N. C. Ismail, "Design and simulation o f self-running magnetic motor," Journal of Engineerin g Technology, vol. 5, pp. 27–31.
15. ^ P. Kelly, "A Practical Guide to Free-Energy devices," 2 010.
16. ^ F. S. Fakhrurrazey, W. N. W. A. Munim, and Z. Oth- ma n, "Performance comparison of 4-pole neodymium m agnet Bedini SSG free energy generator", IEEE 8th Inte rnational Power Engineering and Optimization Confe rence (PEOCO2014), pp. 573–578, 2014.
17. ^ R. Kumar, and R. R. Poojari, "Bedini wheel using elect romagnetic flux generation," Intl. Eng. J. For Research & Development, vol. 2, no. 2, pp. 5–5, 2016.
18. a, b C. Photong, A. Thongnuch, P. Hemkun, and P. Suyoi, "Effects of stationary coil size on capability of electrici ty generation of Bedini generator," Mahasarakham Int l. J. of Eng. Tech., vol. 2, no. 2, pp. 6–10, 2016.
19. ^ U. Sriphan, P. Kerdchang, R. Prommas, and T. Bunnan g, "Coefficient of performance of battery running and charging by magnet generator Bedini," J. of Electroche mical Energy Conversion and Storage, vol. 15, no. 4, 20 18.
20. ^ M. Hidayat, R. Santoso, I. Syamsiana, A. Setiawan, an d S. Djulihenanto, "Design and analysis of a radiant ch arger using 5 coils and 5 poles of neodymium magnet as a rotor drive," J. of Phys. (Conf. Series), vol. 1402, no. 3, p. 033100, 2019.
21. ^ O. Kerimov, N. Tabataei, and N. Rahmanov, "Magneti c DC motor with partially supplied by energy from vac uum," Int. J. Tech. Phys. Probl. Eng, vol. 7, no. 24, pp. 32 –36, 2015.
22. ^ A. E. Chubykalo and R. Smirnov-Rueda, "Convection displacement current and generalized form of maxwel l–lorentz equations," Modern Physics Letters A, vol. 12, no. 01, pp. 1–24, 1997.
23. ^ A. I. Arbab, "On the new gauge transformations of m axwell's equations," Progress in Physics, p. 14, 2007.
24. ^ T. Lee, "Particle physics and introduction to field theo ry, contemporary concepts in physics vol. 1," Harwood Academic, 1981.
25. ^ C. Photong, "Effects of inductive coil turns on voltage generation from low frequency vibrations," IEEE Conf. TENCON, pp. 1–4, 2015.
26. ^ P. T. Krein, "Elements of Power Electronics," 1998.
27. ^ T. Ayodele, A. Ogunjuyigbe, and N. Oyelowo, "Hybridi zation of battery/flywheel energy storage system to i mprove ageing of lead-acid batteries in PV-powered a pplications," Intl. J. of Sustainable Eng., pp. 1–23, 2020.
28. ^ Y. Tong, T. Kozai, N. Nishioka, and K. Ohyama, "Green house heating using heat pumps with a high coefficie nt of performance (cop)," Biosystems engineering, vol. 106, no. 4, pp. 405–411, 2010.
29. ^ M. E. Emetere, U. Okoro, B. Etete, and G. Okunbor, "Fre e energy option and its relevance to improve domestic energy demands in southern Nigeria," Energy Reports, vol. 2, pp. 229–236, 2016.

Declarations

doi.org/10.32388/OS9V96.2

Funding: No specific funding was received for this work.
Potential competing interests: No potential competing interests to declare.

doi.org/10.32388/OS9V96.2